PNAS

Bistable metamaterial for switching and cascading elastic vibrations

Osama R. Bilal[a,b,c,1], André Foehr[b,c], and Chiara Daraio[c,1]

[a]Institute of Theoretical Physics, ETH Zurich, 8093 Zurich, Switzerland; [b]Department of Mechanical and Process Engineering, ETH Zurich, 8092 Zurich, Switzerland; and [c]Division of Engineering and Applied Science, California Institute of Technology, Pasadena, CA 91125

Edited by Rajeev Ram, Massachusetts Institute of Technology, Cambridge, MA, and accepted by Editorial Board Member Evelyn L. Hu March 17, 2017 (received for review November 3, 2016)

The realization of acoustic devices analogous to electronic systems, like diodes, transistors, and logic elements, suggests the potential use of elastic vibrations (i.e., phonons) in information processing, for example, in advanced computational systems, smart actuators, and programmable materials. Previous experimental realizations of acoustic diodes and mechanical switches have used nonlinearities to break transmission symmetry. However, existing solutions require operation at different frequencies or involve signal conversion in the electronic or optical domains. Here, we show an experimental realization of a phononic transistor-like device using geometric nonlinearities to switch and amplify elastic vibrations, via magnetic coupling, operating at a single frequency. By cascading this device in a tunable mechanical circuit board, we realize the complete set of mechanical logic elements and interconnect selected ones to execute simple calculations.

phonononic metamaterials | tunable materials | phonon switching and cascading | phononic computing | acoustic transistor

The idea of realizing a mechanical computer has a long established history (1). The first known calculators and computers were both mechanical, as in Charles Babbage's concept of a programmable computer and Ada Lovelace's first description of programing (2). However, the discovery of electronic transistors rapidly replaced the idea of mechanical computing. Phononic metamaterials, used to control the propagation of lattice vibrations, are systems composed of basic building blocks, (i.e., unit cells) that repeat spatially. These materials exhibit distinct frequency characteristics, such as band gaps, where elastic/acoustic waves are prohibited from propagation. Potential applications of phononic metamaterials in computing can range from thermal computing (3–5) (at small scales) to ultrasound and acoustic-based computing (6, 7) (at larger scales). Phononic devices analogous to electronic or optical systems have already been demonstrated. For example, acoustic switches (8, 9), rectifiers (10, 11), diodes (12–15), and lasers (16, 17) have been demonstrated both numerically and experimentally. Recently, phononic computing has been suggested as a possible strategy to augment electronic and optical computers (18) or even facilitate phononic-based quantum computing (19, 20). All-phononic circuits have been theoretically proposed (21, 22) and phononic metamaterials (23–26) have been identified as tools to perform basic logic operations (6, 7). Electromechanical logic (27) and transistors (28) operating using multiple frequencies have also been demonstrated. Most of these devices operate using electronic signals (26) and/or operate at mixed frequencies. When different frequencies are needed for information to propagate, it becomes difficult, if not impossible, to connect multiple devices in a circuit.

Electronic transistors used in today's electronic devices are characterized by their ability to switch and amplify electronic signals. Conventional field-effect transistors (FETs) consist of at least three terminals: a source, a drain, and a gate. The switching functionality takes place by applying a small current at the gate to control the flow of electrons from the source to the drain. Due to the big difference between the low-amplitude controlling signal (in the gate) and the higher amplitude controlled signal (flowing from the source to the drain), one can cascade an electronic signal by connecting multiple transistors in series to perform computations. In this work, we experimentally realize a phononic transistor-like device that can switch and amplify vibrations with vibrations (operating in the phononic domain). Our phononic device uses elastic vibrations at a gating terminal to control transmission of elastic waves between a source and a gate, operating at a single frequency ($f_0 = 70$ Hz; *Materials and Methods* and *Supporting Information*). It consists of a one-dimensional array of geometrically nonlinear unit cells (representing the metamaterial), connecting the source to the drain (Fig. 1*A*). Each unit cell is composed of a spiral spring containing a magnetic mass at its center. The magnetic mass allows the stiffness of the spiral spring to be tuned by an external magnetic field. The metamaterial is designed to support a resonant, subwavelength band gap, whose band edges vary with the stiffness of the spiral springs (Fig. 1*B*). To tune the mechanical response of the metamaterial, we place an array of permanent magnets under the unit cells. We couple the permanent magnets to a driven, magnetic cantilever (herein referred to as the gate, Fig. S1), designed to resonate at a frequency $f_0 = 70$ Hz. When the gate is excited by a relatively small mechanical signal, the resonance of the cantilever shifts the array of magnets (Movie S1) and tunes the transmission spectrum of the metamaterial (Fig. 1 *B* and *C*). The energy potential of the gating system is bistable (Fig. S2) and provides control of the transmission of a signal from the source to the drain (Fig. S3). We characterize the transistor-like device experimentally (*Materials and Methods* and *Supporting Information*) by fixing one end of the metamaterial structure to the source

Significance

One of the challenges in materials physics today is the realization of phononic transistors, devices able to manipulate phonons (elastic vibrations) with phonons. We present a realization of a transistor-like device, controlled by magnetic coupling, which can gate, switch, and cascade phonons without resorting to frequency conversion. We demonstrate all logic operations for information processing. Because our system operates at a single frequency, we use it to realize experimentally a phonon-based mechanical calculator. Our device can have a broad impact in advanced acoustic devices, sensors, and programmable materials.

Author contributions: O.R.B. and C.D. designed research; O.R.B. and A.F. performed research; O.R.B., A.F., and C.D. analyzed data; and O.R.B., A.F., and C.D. wrote the paper.

The authors declare no conflict of interest.

This article is a PNAS Direct Submission. R.R. is a guest editor invited by the Editorial Board.

[1]To whom correspondence may be addressed. Email: daraio@caltech.edu or bilalo@ethz.ch.

This article contains supporting information online at www.pnas.org/lookup/suppl/doi:10.1073/pnas.1618314114/-/DCSupplemental.

APPLIED PHYSICAL SCIENCES

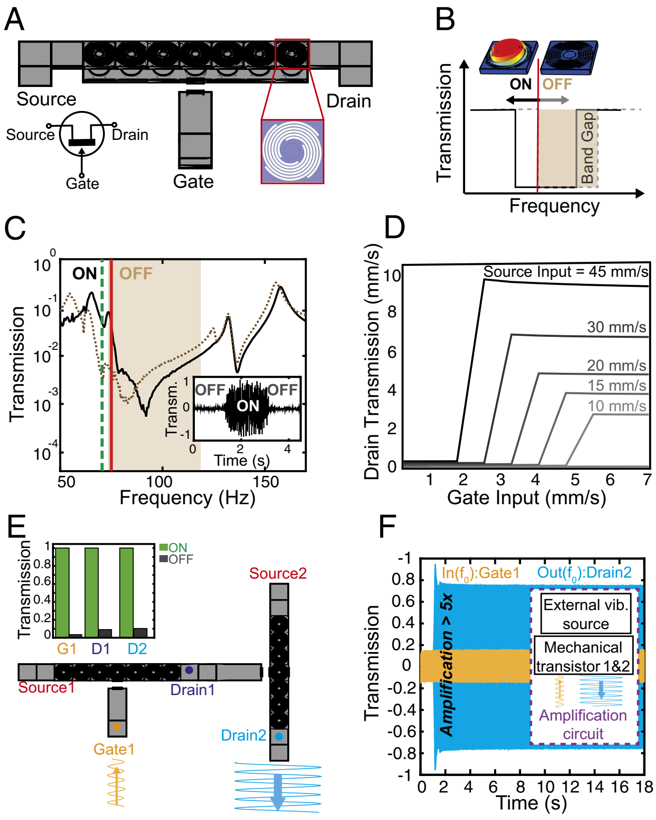

Fig. 1. Phononic switching and cascading. (*A*) Schematic diagram of our device, including a zoom-in view of a unit cell. *A*, *Inset* shows the analogy with a typical FET electronic device. (*B*) Conceptual visualization of the switching principle. As the unit cell shape changes, the transmission spectrum of the signal through the metamaterial shifts between ON/OFF states. The shaded area highlights the band gap in the OFF configuration. (*C*) Experimental transmission spectrum of the transistor in the ON (solid black line) and OFF (brown dotted line) states. *C*, *Inset* shows a time series of the mechanical signal at the operational frequency (marked by the green dashed line). (*D*) Transistor as a switch: experimental measurement of the transmission at the drain as a function of gate input, for different source input. (*E*) Transistor as an amplifier: two connected transistors with *Inset* showing the relative measured signal amplitudes when gate 1 is OFF (gray) and ON (green). (*F*) Experimental time series of the signal measured at gate 1 and drain 2. *F*, *Inset* shows the circuit in analogy to electronics.

(i.e., a mechanical shaker) and the other end to the drain (a fixed, rigid support). The signal at the drain is measured using a laser Doppler vibrometer. The operation frequency of the transistor is indicated by the dashed-green line in Fig. 1*C*. The gate tunes the transmission signal from the source to the drain, acting as a switch for a harmonic, elastic wave with frequency f_0. In Fig. 1*C*, the black and brown transmission lines represent 0 and 1 states and the highlighted orange region is the band gap obtained from the numerical analysis of the infinite periodic medium theory, as in Fig. S4. The ratio between transmission coefficients in the ON and OFF states is 12.5 in Fig. 1*C*. Whereas most transistors retain asymmetric transmission, transistor models (e.g., junction gate field-effect transistor) exist that require one to choose, before using them, which terminal to assign to a drain and a source (i.e., it is symmetric with respect to transmission from the source and the drain). Moreover, if an asymmetric transmission is required, a defect can be simply incorporated into the metamaterial array (15); however, this might come at the expense of operating at a unified single frequency (because of the nonlinear mode conversion).

To demonstrate the switching functionality of the transistor, we measure the transmission at the drain as a function of gate input (Fig. 1*D*). As we increase the vibration amplitude at the source, we observe an increase in the efficiency of the transistor as a switch. For instance, when the source input is relatively small, e.g., the velocity amplitude of the driving signal is set to 15 mm/s, the gate can be opened (switching the system ON) with a gate excitation of 5 mm/s, with a source-to-gate input ratio of 3. If the source input is larger, e.g., 45 mm/s, a smaller excitation of the gate, 3 mm/s, is sufficient to switch the system ON, with a source-to-gate input ratio of 15. Stronger source signals translate to larger displacements of the metamaterials that, in turn, affect the coupling strength between the array of control magnets and the magnets in the metamaterial. The strengthening of this coupling leads to an increase in efficiency in the gating functionality, defined as source-to-gate input, by at least a factor of 5 in the configurations tested experimentally.

To demonstrate signal cascading, we connect two transistors in a mechanical circuit (Fig. 1*E*). During the experiments, the sources of both transistors (sources 1 and 2) are always turned ON, and the transmission at gate 1, drains 1 and 2 is measured with a laser vibrometer (Fig. 1*E*). We normalize the signal at both drain terminals to its maximum amplitude of transmission, to visualize the difference between the ON and OFF states. The leakage at the two drain terminals is less than 10% of the transmission amplitude when the gate is closed (Fig. 1*E*, *Inset*). This value is close to the background noise level captured by the laser vibrometer in absence of excitation. To show the cascading effect between the two transistors, we consider the time signal of gate 1 as the circuit input and the measured signal at drain 2 as the circuit output (Fig. 1*F*). Once gate 1 is open, both drain 1 and drain 2 gain transmission, with a delay of less than 1 s. The two signals (drain 2 output)/(gate 1 input) demonstrate an amplification factor bigger than 5. This value can be increased by changing the excitation amplitude of source 2.

Modern electronic devices use connected stacks of switches to perform logic operations. For example, in an AND logic operation, when two switches are connected in series, no signal passes through unless both switches are open. In other words, the output of the circuit is 1 (true) when both inputs are 1 (true) and 0 (false) otherwise. If two switches are connected in parallel, when either one of them is open (true), the circuit produces an output signal (true). This circuit represents an OR gate. Following the same approach, one can create all of the basic electronic logic gates, using switches as basic building blocks (Fig. S5). In our work, we use a configuration of four interconnected switches to experimentally realize phononic logic gates analogous to all existing electronic ones. We refer to this configuration as the universal phononic logic gate (UPLG) (Fig. 2*A*). One terminal (Fig. 2*A*, *Left*) of the UPLG is connected to a vibration source that excites harmonic elastic waves. We measure the signal transmitted to the other terminal (Fig. 2*A*, *Right*) in the location indicated by the blue and orange dots. To implement all of the logic operations, we change the coupling between the magnetic control stages (M_i, with $i = 1,...,4$) for each gate in a systematic manner (Fig. 2*B*). For instance, to have an AND gate, we connect M_1 and M_3 into one magnetic stage that could be driven by a magnetic cantilever as a single control unit, representing a binary state, A. Stages M_2 and M_4 are coupled in a similar manner representing another binary state, B. The positions of the magnetic stages, resembling the AND gate functionality, represent the logic operation 0 AND 0 resulting in 0 (i.e., all switches are black/OFF, Fig. 2*B*). Another example is the XNOR gate; both pairs $M_{1,3}$ and $M_{2,4}$ are coupled, but with a different coupling distance than the AND gate. The XNOR represents the operation 0 XNOR 0 that results in 1 (two green/ON switches along the same transmission line, Fig. 2*B*). The numerical simulations of the operations 1 UPLG

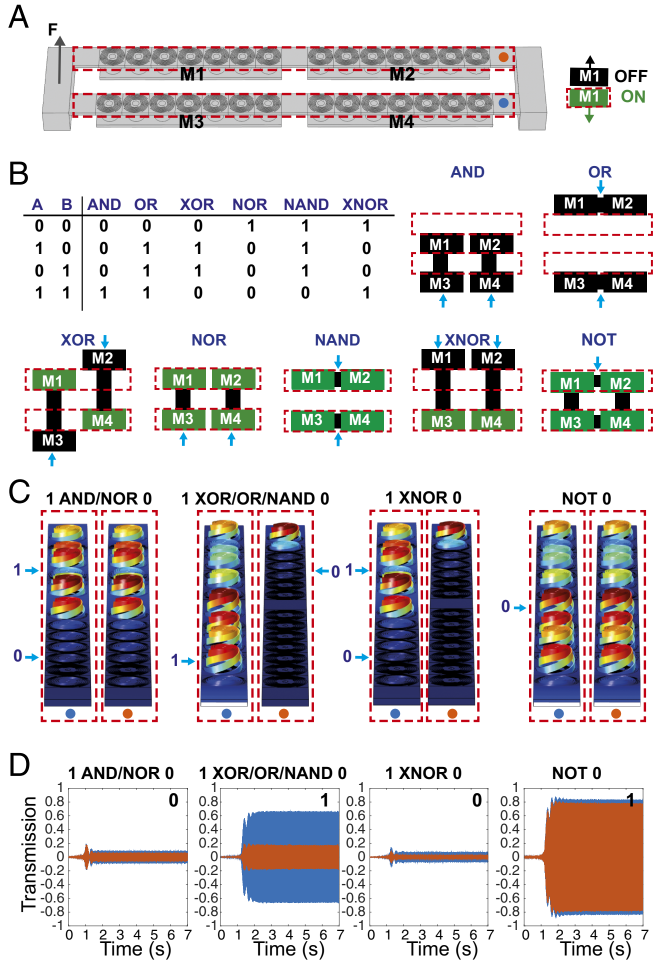

Fig. 2. Phononic logic gates. (*A*) Schematic of four interconnected switches. (*B*) Schematic of the relative positions of the magnetic stages in reference to the metamaterial for the logic gates representing the first row in the table (A = 0 and B = 0). The NOT gate operates on a single input (A = 0). (*C*) Numerical simulations of the different logic gates representing the second row in the table in *B*. (*D*) Experimental time series for different gates. Orange and blue curves correlate with the dots in *A* and *C*. The red, dashed lines in *A*–*C* are the reference frames for the magnetic control stages M_{1-4}. The green/ON and black/OFF represent the position of the stage, relative to the metamaterial. The magnetic stage is either underneath the spiral springs (ON) or displaced laterally by 6 mm (OFF). The cyan arrows represent the logical inputs A and B. The vibration source powering the logic gates with the harmonic excitation F is always on.

0 (Fig. 2*C*) agree with the corresponding experimental measurements (Fig. 2*D*). In experiments, we measure the output at the two end points of the UPLG, to characterize each transmission line and define the output of the gate as the summation of the two signals. We define logical 1 as signals with a transmission amplitude bigger than two-thirds of the maximum signal transmitted through 14 resonators (one line of resonators in Fig. 2*A*) and logical 0 as signals with less than one-third of that maximum. For example, for the logic operation 1 OR 0 (Fig. 2*D*, *Center Left*) one transmission line is open (blue) whereas the other is closed (orange). In this case, we measure about 10% transmission leakage from the ON to the OFF line.

The realization of all logic gates is the basis for performing computations in various devices. In a binary calculator for example, the addition operation is executed in the calculator circuit board by a group of contiguous full adders (Fig. 3*A*). The number of binary bits a calculator can add is equivalent to the number of full adders it contains. Each of these adders can be split into two half adders, each composed of interconnected XOR and AND gates (Fig. 3*B*). The circuit board for a mechanical full adder composed of two half adders (Fig. 3*C*) is similar to an electronic calculator, in which the two half adders are linked together by an OR gate. We experimentally construct the phononic circuit board for a simple binary calculator. We demonstrate, without any loss of generality, the calculator carrying out the operation 1 + 1. To add two bits, only a single half adder is needed (there is no carry-in from any previous operation). The experimentally obtained time-series envelope of the operation 1 + 1 is presented in Fig. 3*G*. Fig. 3*D* shows the mechanical signal as it propagates in the circuit in red lines, whereas the attenuated signal is plotted in black lines. The difference between the transmitted vs. the attenuated signal is more than one order of magnitude, drawing a distinct line between the 0 and 1. The finite-element mode shapes (Fig. 3*E*) of the same operation agree with the measured transmission pathway. The realization of a circuit board for a full-fledged mechanical calculator (addition, subtraction,

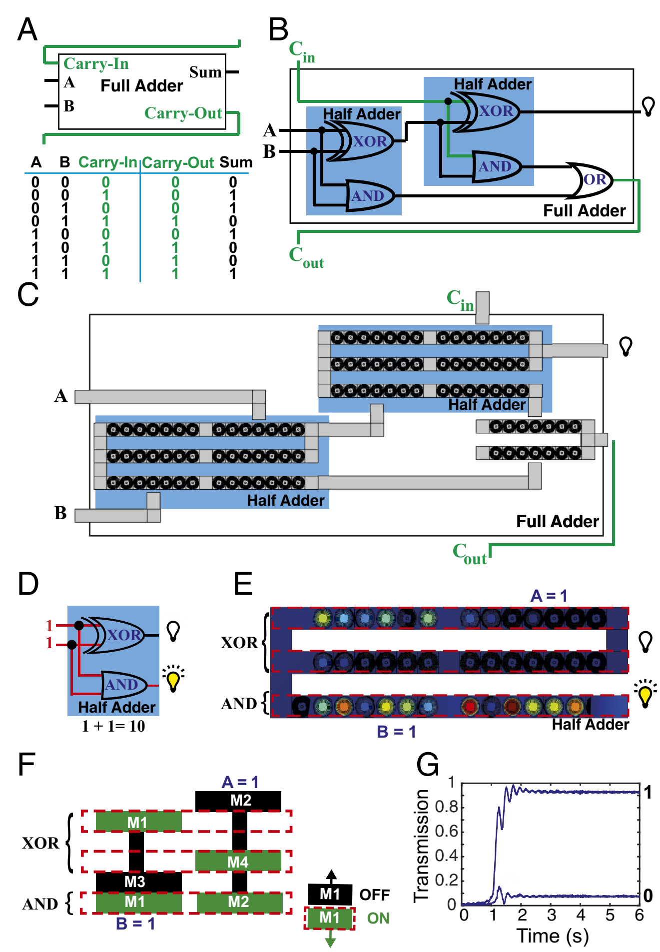

Fig. 3. Phononic calculator. (*A*) Schematic of the input/output signals in a full adder with its truth table. (*B*) Detailed schematic of the full adder broken down into its basic logic elements. (*C*) Schematic of the mechanical analogues full adder composed of two phononic half adders. In *A*–*C*, green lines indicate a signal between two different interconnected full adders. (*D*) Schematic of a half adder with logical inputs (A = B = 1) indicated by red lines. (*E*) Numerical simulations of a mechanical half adder. (*F*) Schematic of the relative position of the magnetic stages to the metamaterials. (*G*) Experimental time series for the half adder. The transmitted signal is normalized by the maximum transmission amplitude at the measurement (right) end of the phononic half adder. *D*–*G* represent the execution of the operation 1 + 1.

multiplication, and division) using the same design principle can easily follow. Although our proof-of-principle experiments were performed at the macroscopic scale, the planar geometry of our devices makes them scalable to micro/nanoscales. Miniaturization of the concept would allow the realization of devices that operate at higher-frequency ranges and speeds. For instance, if we scale the unit cell size to 25 μm, a dimension easily achievable with conventional microfabrication tools, the device will operate in the ultrasonic frequency range $\sim$70 kHz. The speed of switching will scale by a power of 4 [mass scales approximately $O(3)$ and the distance scales linearly]. This translates to a possible switching speed much higher than the frequency of operation.

This work presents a conceptual design of a dynamically tunable phononic switch and provides experimental realization for its functionality. The connection of multiple elements in a circuit allows it to perform computing operations. This provides an experimental demonstration of switching and cascading of phonons at a single frequency and serves as the basis for mechanical information processing, which can have an impact in soft robotics, programmable materials, and advanced acoustic devices.

Materials and Methods

For the experimental realization of the phononic transistor-like device, the tunable metamaterial, connecting source and drain, was fabricated from medium-density fiberboard (MDF), using a Trotec Speedy 300 laser cutter. The mechanical properties of the MDF were characterized using a standard tensile test with an Instron E3000. The measured Young's modulus is 3 GPa and the density is 816 Kg/m^3. The quality factor of the metamaterial is $\approx$20 (Fig. S6). The unit cells in the metamaterial consist of four concentric and equally spaced Archimedean spirals, with lattice spacing of 25 mm. Cylindrical neodymium nickel-plated magnets, with a 3-mm diameter and a 3-mm thickness, were embedded in the center of each unit cell. An array of control magnets with a 20-mm diameter and 5-mm thickness was placed on a movable stage below the array of unit cells. To control the movable stage, we coupled it to a vibrating cantilever (the gate) attached to a separate vibration source (Fig. 1*A* and *Supporting Information*). The gate is a rectangular cantilever of dimensions 125 mm $\times$ 15 mm, connected to the drain (right end) of the metamaterial. The gate-control magnets, attached to the side of the control stage, are squares, with 10-mm side length and 3-mm thickness, whereas the ones attached to the cantilever are rectangular with 6-mm $\times$ 4-mm $\times$ 2-mm dimensions.

Mechanical oscillations in the source terminal were excited using a Mini-Shaker (Brüel & Kjær Type 4810) with two identical audio amplifiers (Topping TP22) and were then optically detected at the drain by a laser Doppler vibrometer (Polytec OFV-505 with a OFV-5000 decoder, using a VD-06 decoder card). A lock-in amplifier from Zürich Instruments (HF2LI) was used to filter the signal. The frequency response functions plotted in Fig. 1*C* are the velocity amplitude at the output (drain) normalized to the signal at the input (source). The time series in Figs. 1 *C* and *F*, 2*D*, and 3*G* are obtained using an oscilloscope (Tektronix DPO3014). The time signals in Figs. 2*D* and 3*G* are filtered using a passband filter between 50 Hz and 90 Hz. The excitation amplitude at the source is 15 mm/s in Fig. 1*C*. All of the numerical simulations are done in COMSOL 5.1, using the structural mechanics module.

ACKNOWLEDGMENTS. The authors thank Sandeep Deshpande for assisting in the construction of the setup of the signal amplification experiment. The authors acknowledge the fruitful discussions with V. Costanza, R. Di Giacomo, and M. S. Garcia. This work was supported by ETH Postdoctoral Fellowship FEL-26 15-2 (to O.R.B.) and ETH Grant ETH-24 15-2.

1. Freeth T, et al. (2006) Decoding the ancient Greek astronomical calculator known as the antikythera mechanism. *Nature* 444:587–591.
2. Menabrea L (1842) Sketch of the analytical engine invented by Charles Babbage, with notes by the translator Augusta Ada King, Countess of Lovelace. *Taylor Sci Mem* 3:666–731.
3. Li B, Wang L, Casati G (2006) Negative differential thermal resistance and thermal transistor. *Appl Phys Lett* 88:143501.
4. Wang L, Li B (2007) Thermal logic gates: Computation with phonons. *Phys Rev Lett* 99:177208.
5. Joulain K, Drevillon J, Ezzahri Y, Ordonez-Miranda J (2016) Quantum thermal transistor. *Phys Rev Lett* 116:200601.
6. Bringuier S, et al. (2011) Phase-controlling phononic crystals: Realization of acoustic Boolean logic gates. *J Acoust Soc Am* 130:1919–1925.
7. Zhang T, Cheng Y, Guo Jz, Xu Jy, Liu Xj (2015) Acoustic logic gates and Boolean operation based on self-collimating acoustic beams. *Appl Phys Lett* 106:113503.
8. Li F, Anzel P, Yang J, Kevrekidis PG, Daraio C (2014) Granular acoustic switches and logic elements. *Nat Commun* 5:5311.
9. Babaee S, Viard N, Wang P, Fang NX, Bertoldi K (2016) Harnessing deformation to switch on and off the propagation of sound. *Adv Mater* 28:1631–1635.
10. Liang B, Yuan B, Cheng Jc (2009) Acoustic diode: Rectification of acoustic energy flux in one-dimensional systems. *Phys Rev Lett* 103:104301.
11. Liang B, Guo X, Tu J, Zhang D, Cheng J (2010) An acoustic rectifier. *Nat Mater* 9:989–992.
12. Popa BI, Cummer SA (2014) Non-reciprocal and highly nonlinear active acoustic metamaterials. *Nat Commun* 5:3398.
13. Li XF, et al. (2011) Tunable unidirectional sound propagation through a sonic-crystal-based acoustic diode. *Phys Rev Lett* 106:084301.
14. Devaux T, Tournat V, Richoux O, Pagneux V (2015) Asymmetric acoustic propagation of wave packets via the self-demodulation effect. *Phys Rev Lett* 115:234301.
15. Boechler N, Theocharis G, Daraio C (2011) Bifurcation-based acoustic switching and rectification. *Nat Mater* 10:665–668.
16. Vahala K, et al. (2009) A phonon laser. *Nat Phys* 5:682–686.
17. Jing H, et al. (2014) Pt-symmetric phonon laser. *Phys Rev Lett* 113:053604.
18. Sklan SR (2015) Splash, pop, sizzle: Information processing with phononic computing. *AIP Adv* 5:053302.
19. Ladd TD, et al. (2010) Quantum computers. *Nature* 464:45–53.
20. Reinke CM, El-Kady I (2016) Phonon-based scalable platform for chip-scale quantum computing. *AIP Advances* 6(12):122002.
21. Liang B, Kan Ww, Zou Xy, Yin Ll, Cheng Jc (2014) Acoustic transistor: Amplification and switch of sound by sound. *Appl Phys Lett* 105:083510.
22. Malishava M, Khomeriki R (2015) All-phononic digital transistor on the basis of gap-soliton dynamics in an anharmonic oscillator ladder. *Phys Rev Lett* 115:104301.
23. Liu Z, et al. (2000) Locally resonant sonic materials. *Science* 289:1734–1736.
24. Maldovan M (2013) Sound and heat revolutions in phononics. *Nature* 503:209–217.
25. Hussein MI, Leamy MJ, Ruzzene M (2014) Dynamics of phononic materials and structures: Historical origins, recent progress, and future outlook. *Appl Mech Rev* 66:040802.
26. Cummer SA, Christensen J, Alù A (2016) Controlling sound with acoustic metamaterials. *Nat Rev Mater* 1:16001.
27. Mahboob I, Flurin E, Nishiguchi K, Fujiwara A, Yamaguchi H (2011) Interconnect-free parallel logic circuits in a single mechanical resonator. *Nat Commun* 2:198.
28. Hatanaka D, Mahboob I, Onomitsu K, Yamaguchi H (2013) A phonon transistor in an electromechanical resonator array. *Appl Phys Lett* 102:213102.
29. Levitt MH (2001) *Spin Dynamics: Basics of Nuclear Magnetic Resonance* (Wiley-VCH, Chichester, UK).
30. Bilal OR, Hussein MI (2013) Trampoline metamaterial: Local resonance enhancement by springboards. *Appl Phys Lett* 103:111901.